Materials and Process Study for Polymer Hybrid Bonding

Masaya Jukei, Kota Nomura, Yugo Tanigaki, Takenori Fujiwara, Hitoshi Araki,Tomoyuki Honda and Yu Shoji
Electronic & Imaging Materials Research Laboratories, Toray Industries, Inc.

1-2, Sonoyama 3-chome, Otsu, Shiga, 520-0842 Japan
Ph: +81-77-533-8083; Fax: +81-77-533-8707
Email: masaya.jukei.n6@mail.toray

Abstract
Low-temperature curable polyimides with minimal device damage have been developed for 3D stacking organic hybrid bonding technology. We confirmed developed polyimides showed significant polishing rates for alkaline slurry. Polyimide-to-polyimide bonding and polyimide/copper hybrid bonding at a low-temperature annealing were successfully demonstrated. Furthermore, polyimide-to-polyimide bonding mechanisms were investigated from the chemical and physical aspects of the material, respectively. Moreover, polymer hybrid bonding with copper protrusion test vehicles was successfully polished with Chemical Mechanical Polishing, which showed good polyimide-to-polyimide and copper-to-copper joints. Finally, it was confirmed that they could maintain insulation reliabilities after accelerated tests.

Key words
Chip-to-wafer, low-temperature process, polyimide, polymer hybrid bonding

I. Introduction
In recent years, the input/output (I/O) density of semiconductor packages has increased significantly due to higher-performance semiconductors and higher chip integration, such as high-performance computing (HPC) and memory stacking applications ([1]-[3]). As I/O density increases, the pitch of electrodes becomes narrower, and conventional solder bump bonding is no longer applicable. Hybrid bonding is currently being investigated as an alternative to solder-die interconnect with a wiring pitch of 15 μm or less for higher I/O density integration [4].

Hybrid bonding is divided into two main types, which are wafer-to-wafer (W2W) and chip-to-wafer (C2W) bonding. W2W hybrid bonding technology is a maturing process for CMOS image sensors and NAND Flash memory, but it is less flexible than C2W since it requires the chips to be the same size, and it is not always possible to bond good chips together (cumulative yields should be low). C2W hybrid bonding technology is being developed to implement multiple semiconductor chips to the substrate for heterogeneous integration packages ([5],[6]). The advantages of C2W are: 1) Select known good die (KGD), 2) bond different size chips, and 3) stack multi chips. One of the difficulties of C2W hybrid bonding based on SiO_2 dielectric in terms of package reliability is warpage caused by 3D stacking of thin chips with high internal stress inorganic layers. Furthermore, defects caused by void generation from dicing dust particles at the interface due to high modulus of SiO_2 is also an issue. In addition to the difficulties, the high-temperature bonding process for SiO_2 may face another issue for temperature-sensitive devices such as memory devices.

On the other hand, hybrid bonding technology using organic polymers is expected to suppress the internal stress as a stress buffer layer and the generation of voids because of the lower modulus than SiO_2; therefore, it can be considered as one of the key solutions. In addition, low-temperature bonding and annealing processes are heavily correlated in preventing temperature-sensitive devices from thermal damage during module integration. Knowing the robust mechanical and thermal properties of polyimides (PIs), these polyimide materials must be the best-fit materials for hybrid bonding.

In this work, low-temperature processable PIs as organic insulating materials have been evaluated for organic C2W hybrid bonding. Low-temperature curable PIs, which need a higher polishing rate than 500 nm/min for CMP and lower than 250 ºC for the bonding process, were prepared to apply them to low-temperature 3D stacking process. In this case of the low-temperature PI-PI bonding test, we confirmed higher bond strength compared to SiO_2-SiO_2 without the absence of voids in submicron order. Moreover, Surface Free Energy (SFE) and X-ray Photoelectron Spectroscopy (XPS) analysis for PI-coated Si substrate after plasma activation treatment

was also conducted to examine the physicochemical state of the PI surface before the bonding process and identify the mechanism of PI-PI bonding. Furthermore, Cu protrusion with PI dielectric test vehicles was successfully polished with Chemical Mechanical Polishing (CMP) and bonded to complete the C2W process. Finally, to confirm applicability to semiconductor packages, the insulation reliabilities of PI were examined by biased highly accelerated stress test (B-HAST).

II. Experimental Section

A. Preparation of polymer

The PI precursor was synthesized by reacting diamines with tetracarboxylic dianhydrides in a solvent under N_2 gas flow. After the reaction, the reaction mixture was poured into water and washed several times, and then the precipitation was collected and dried at 50 ºC for 3 days to obtain the PI precursor. Then, the dried PI precursor and some commercial additives were mixed into solvents such as ɤ-butyrolactone or N-methylpyrrolidone. The solution was filtered through a 0.2 µm pore poly(tetrafluoroethylene) filter to eliminate the particles.

B. Evaluation of polyimide

Mechanical properties of PI films, such as tensile strength, Young's modulus, and elongation, were measured on a universal tester (TENSILON RTM-100, A&D Manufacturing Company) at a tensile speed of 5 mm/min.
Thermal analysis of films was obtained from a thermal analyzer (EXSTAR 6000 TMA/SS6100, Seiko) at a heating rate of 5 °C/min for coefficient of thermal expansion (CTE) and glass transition temperature (Tg) measurement.

C. General PI-PI bonding test

Bond strength was evaluated with die shear tester. Samples for tests were fabricated by the process as shown in Fig. 1. The PI varnish was coated on 200 mm Si wafers by a spin-coater (ACT-8, Tokyo Electron), and prebaked at 120 °C for 3 min on a hot plate, then cured in a clean oven (CLH-21CD (V)-S, KOYO THERMOSYSTEMS) at a condition of less than 250 °C for 60 min under N_2 purged atmosphere. After curing, the wafers were singulated into 2.5×2.5 mm chips or 6×6 mm chips (top chip), and 12×12 mm chips (bottom chip), respectively, using a dicing saw (DAD3350, Disco). The diced chips were treated to activate the PI surface in the Ar atmosphere by plasma etcher (PC-100B+H, Hitachi High-Tech Instruments). After surface activation, each top chips were pre-bonded to the bottom chips using a flip-chip bonder (FC3000WS, Toray Engineering). These samples were annealed in a clean oven (CLH-21CD (V)-S, KOYO THERMOSYSTEMS) at a condition of 250 °C for 60 min under N_2 purged atmosphere. Then, a die shear test was conducted by a bond tester (Dage Series 4000, Nordson Advanced Technology).
The state of PI-PI bonding interfaces was observed by cross-sectional Scanning Electron Microscope (FE-SEM S-4800, Hitachi) and Scanning Transmission Electron Microscope (ARM 200F Dual-X, JEOL) images.

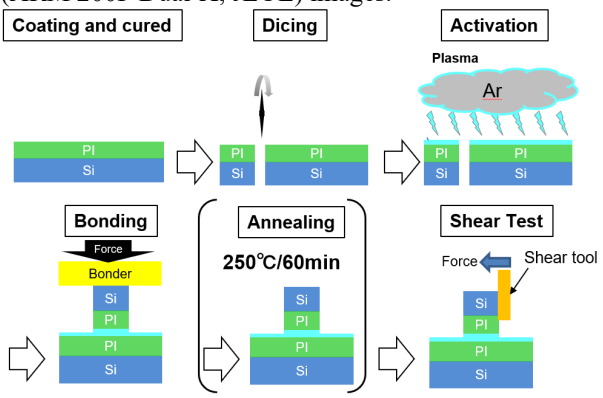

Fig.1 Process of general PI-PI bonding test.

D.Analysis of PI-PI bonding mechanism

Surface Free Energy (SFE) and surface chemical state of PI coated Si chip after plasma activation treatment were measured by contact angle meter (DMo-701, Kyowa Interface Science) and X-ray Photoelectron Spectroscopy (XPS) analysis (Quantera SXM, Ulvac-PHI) respectively.
Elastic modulus of PI-A and PI-B films were measured at room temperature (rt), 100 °C, 150 °C, 200 °C and 250 °C using the nanoindentation method (Nano Indenter G200X Inforce 1000, KLA).

E. CMP process

The CMP process for PI was conducted by the CMP tool (Mirra 200 mm, APPLIED MATERIALS).
Another CMP process for Cu/PI hybrid bonding was also done by a table-top lapping machine (NF-300, NANO FACTOR) at lower than 40 °C. In this process, alkaline type slurry and hard type pad were used.

F. Reliability test on B-HAST

The polyimide solution was coated at 10 µm thickness on the TEG substrate. The dimensions of line/space and height of copper were 2 µm / 2 µm and 3 µm, or 5 µm / 5 µm and 3 µm, respectively. Then, B-HAST was carried out at 130 °C in 85 %RH.

III. Results and discussion

A. Concept of polymer development

At first, for the purpose of this study on hybrid bonding, several types of polyimides that can be cured at low temperatures of 250 °C or less were designed. In designing materials, low-temperature processable feature was achieved by low-temperature imidization technology. At first, the CMP polishing rate of each designed material, which has several types of PI backbone and composition, was investigated. As a result, it was found that polishing rates varied from 330 to 700 nm/min depending on the PI materials. In this study, two types of PIs that had fast polishing rates and different characteristic properties were specifically focused on.

Polyimide A (PI-A) is a low elasticity type suitable for room temperature or lower pressure bonding. On the other hand, polyimide B (PI-B) has a low CTE characteristic. The mechanical and thermal properties of the two types of polyimides are shown in Table I. PI-A exhibits an elongation of 100% under condition of 230 °C curing and demonstrates high toughness suitable for multilayer stacking. On the other hand, PI-B has a CTE of 23 ppm/K, which is close to that of copper (18 ppm/K). This similarity in CTE can contribute to providing high reliability in the package after stacking.

Table. I General properties of PIs

Properties		PI-A	PI-B	PI-C	PI-D	PI-E
Curing condition	℃/min	230/60	250/60	230/60	220/60	230/60
Tensile	MPa	120	140	103	150	132
Elongation	%	100	68	78	110	25
Young's modulus	GPa	1.7	3.2	2.1	2.0	2.1
CTE	ppm/K	68	23	71	55	51
Tg	℃	150, 280	283	257	245	278
CMP rate	nm/min	700	700	330	550	450

B. PI-PI bonding

1) Bonding strength

For applications, such as memory devices, which are sensitive to thermal treatment during the bonding process, it is preferred to conduct the bonding process at a low temperature. In addition, it is also desirable to perform a constraint on pressure during the bonding process, making it preferable to perform bonding at as low pressure as possible. The critical values of the necessary bonding temperature and pressure to obtain high bonding strength were investigated by adjusting the bonding pressure and bonding temperature using PI-A and PI-B. The results of the bond strength at bonding temperatures of 40 ºC to 250 ºC and annealing temperatures of 250 ºC are shown in Fig. 2. From the results in Fig. 2, sufficient bonding strengths (die shear strength of over 25 MPa) were confirmed at certain conditions, and all processes were carried out at 250 °C or less for both PIs. PI-A demonstrated exceptional bond strength of over 25 MPa under the conditions of 0.35 MPa of pressure at 150 ºC and 8.0 MPa of pressure at 40 ºC, respectively. On the other hand, PI-B exhibited exceptional bond strength of over 25MPa under the conditions of 1.6 MPa/200 ºC and 8.0 MPa/80 ºC. The increase in temperature and pressure tends to enhance the bond strength, and the critical values of temperature and pressure necessary to achieve sufficient bond strength were confirmed. Thus, the trade-off relationship between bonding pressure and temperature was implied. Moreover, differences in critical values were observed between PI-A and PI-B. For example, the required bonding temperatures at 8.0 MPa bonding pressure were <40 °C for PI-A and 80 °C for PI-B, respectively. PI-B required a higher bonding temperature compared to PI-A. Therefore, it is considered that the necessary bonding temperature and pressure may depend on the type of PIs.

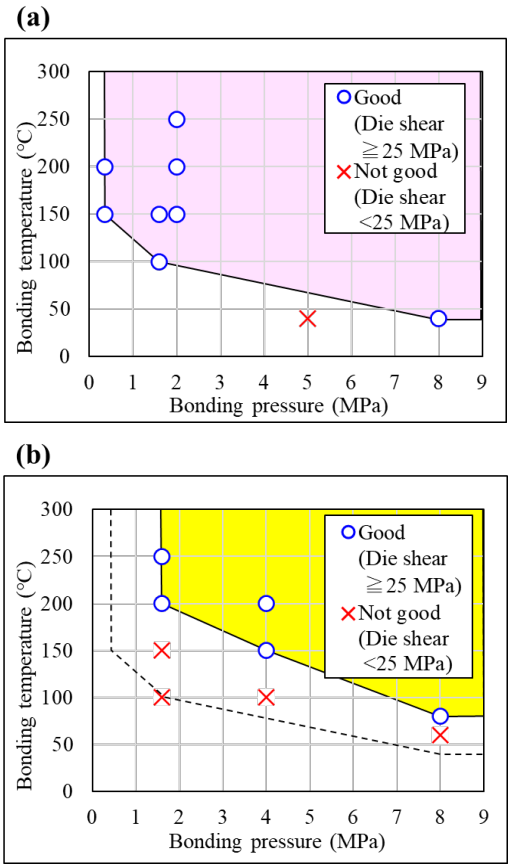

Fig. 2 Bonding strengths obtained from different bonding temperatures and pressures for (a) PI-A and (b) PI-B, ○: Good die shear strength, ×: Not good die shear strength.

2) PI-PI bonding interface

Furthermore, PI-PI bonding interfaces were observed by FIB-SEM and STEM. Fig. 3 shows the cross-section image of the interface of PI-A bonded under the condition of 8 MPa/40°C. As shown in Fig. 3, it was confirmed that the interface could be bonded and no submicron-scale void was observed.

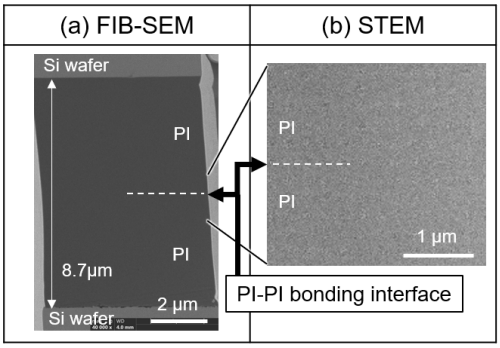

Fig. 3 Cross-section images for PI-PI bonding interface, (a) FIB-SEM and (B) STEM images.

C. Bonding mechanism

1) Effects of surface activation by plasma treatment

It is known that high bond strength can be realized by activating the surface of polyimide through plasma treatment before compressing. In this study, the effects of surface activations by plasma treatment and the mechanism of PI-PI bonding were investigated. First, the physicochemical effects on the surface state by plasma treatment were evaluated through surface free energy measurement. The contact angles of water, formamide, diiodomethane, and ethylene glycol against PI surfaces were measured at room temperature, and the component of the solid surface free energy was calculated by the extended Fowkes equation [7]. This method allows for a detailed analysis of the surface chemical status and contributes to a better understanding of the bonding mechanism. As shown in Fig. 4, it was confirmed that the surface free energies for polar and hydrogen bond components after plasma treatment increased compared to without treatment. The same trend was observed in both PI-A and PI-B; therefore, the increase in hydrogen bonding component and polar component is considered to mainly contribute to the bonding process.

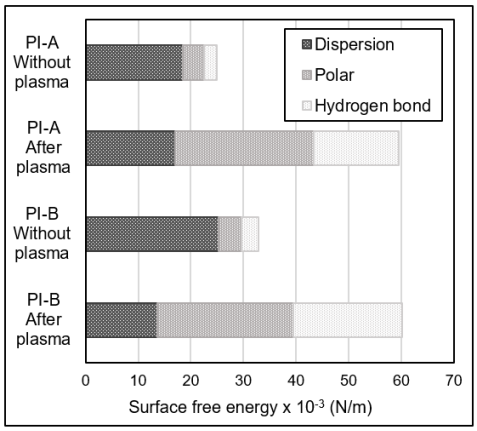

Fig. 4 Effect of plasma activation on polymer surface.

Next, the activation on the PI-B surface after plasma treatment by using XPS measurements was investigated. The result of PI-B is shown in Table II. Table II indicates the increasing ratio of oxygen atoms, nitrogen atoms, and carboxyl groups to carbon atoms. These groups are considered to mainly contribute to the increase in polar component and hydrogen bonding component in surface free energy.

Table II. Ratio of atomic and substituent numbers

Plasma treatment	C	N	O	-COOH
No	1.00	0.03	0.29	0.001
Done	1.00	0.09	0.49	0.013

From these results, a phenomenon occurring at the bonding interface is assumed to be the chemical interaction, as shown in Fig. 5. It was indicated that the initial PI-PI bonding may be produced by hydrogen bond. Due to carboxyl groups and amine groups generated by Ar plasma and subsequently making stronger covalent bonds by intermolecular imidization (not sure of this word) reaction during the annealing process.

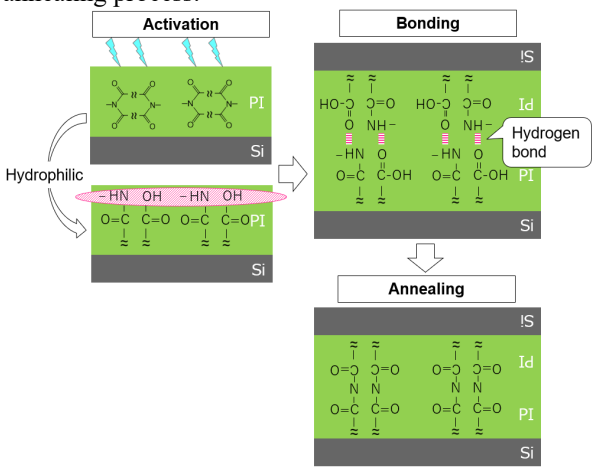

Fig. 5 Assumed mechanism for PI-PI bonding.

2) Analysis of thermodynamic factors

As mentioned in the previous section, since there was almost no significant difference in the surface free energy of PI-A and PI-B, it is considered that the difference in bond strength relies more on another factor, such as physical effects than the influence of chemical bonds. This suggests that the physical properties of the polyimide play an important role in the PI-PI bonding process as well as chemical interaction. To investigate what reason influenced the bondable temperature to vary depending on the type of polyimide, the physical properties of PI-A and PI-B using variable temperature nanoindentation tests were examined. This method can precisely measure the material's mechanical properties under different temperature conditions, and it is important to understand the bonding behaviors of the

polyimides. As shown in Fig. 6, there is a remarkable difference in the elastic modulus with respect to temperature between PI-A and PI-B. For example, PI-B showed an elastic modulus of 4.5 GPa at 150°C, which is almost the same as the elastic modulus of PI-A at room temperature (rt). Through these results, it is safe to say that each polyimide sample reached a certain elastic modulus that allows bonding when it exceeds a specific temperature, suggesting that high bond strength can be achieved for any polymer if the matching temperature can be found. From these results, in order to obtain sufficient PI-PI bonding strength, it was found that it is important to conduct the bonding process with a low elastic modulus.

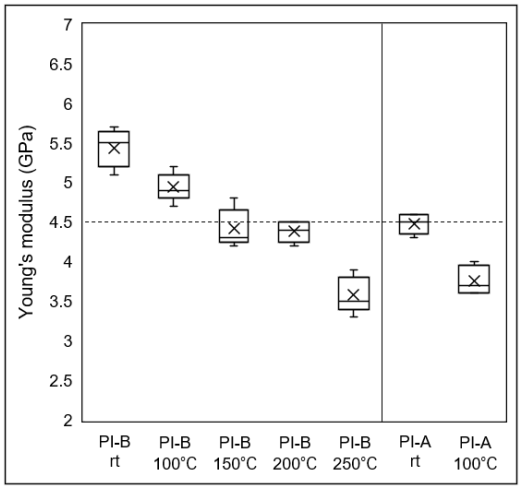

Fig. 6 Nanoindentation results for young's modulus on each temperature.

D. Hybrid bonding

1) Process

The polymer/Cu hybrid bonding process using PI-A for a dielectric material was conducted as the procedure below. PI-A was coated on Si wafer with copper pillars (5 µm, 10 µm pitch). Within this wafer, large chips consisting of 18 small chips (6×13 mm) were singulated to efficiently proceed with the hybrid bonding CMP. Fig. 7 shows details of hybrid bonding chip information. Next, large diced chips were fixed at the center of the wafer-like substrate. Finally, it was polished with CMP. After polishing, two center small chips were observed.

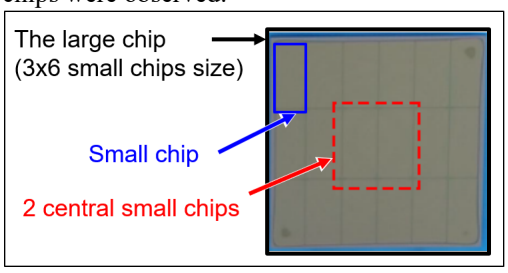

Fig. 7 Detailed hybrid bonding chip information.

2) Controlling copper protrusion by CMP

As a result of CMP, the chips shown in Fig. 8(a), two central small chips were precisely polished. The surface status of PI and Cu were examined with AFM analysis (Fig. 8(b)), which confirmed the Cu protrusions to be within the target of 5 nm (Table III).

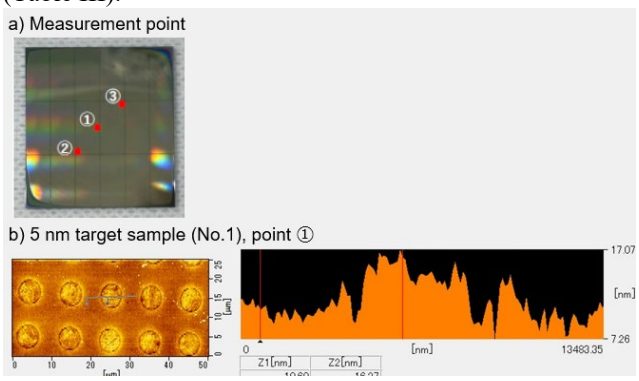

Fig. 8 Surface profile of hybrid bonding chips by AFM analysis (a) measurement points, (b) 5 nm Cu protrusion target.

Table III. Amount of copper protrusion

Target	No.	①	②	③
5 nm	1	+5.7 nm	+5.4 nm	+8.3 nm
	2	+3.4 nm	+3.9 nm	+3.9 nm

3) Cross Section view of hybrid bonding

After CMP, polished center small chips were bonded with the following conditions: Chuck table temperature at rt, and the arm temperature at 200ºC. The compressing force was 25 N (0.35 MPa) for 3 s, and annealing at 250 ºC/3 hr. After annealing bonded chips, the bonding interfaces of chips were observed by SEM. Fig. 9 shows the cross-section SEM image of chip No. 1, which has 5 nm Cu protrusion. Good PI-PI and Cu-Cu joints without voids were observed. Thus, PI/Cu hybrid bonding without voids at the bonding interface was successfully demonstrated.

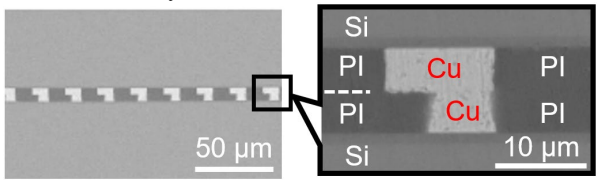

Fig. 9 Cross section SEM image for chip No.1 with 5 nm Cu protrusion.

E. Reliability test results of PI-A and PI-B

To be used as a dielectric layer of hybrid bonding, PI-A and PI-B must have good insulation abilities after reliability tests. Their electric reliability results by B-HAST are shown in Fig. 10.

PI-A and PI-B showed good insulation reliabilities after B-HAST tests in each condition. These results indicated that PI-A and PI-B have enough insulating performance as dielectric layers for hybrid bonding even after the reliability test.

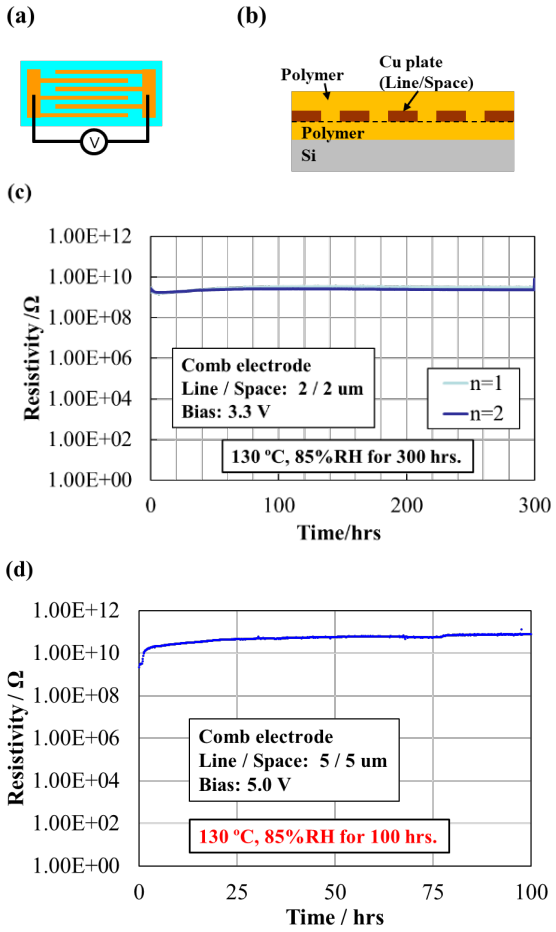

Fig. 10 (a) Top of view of the test vehicle, (b) cross-section view of a test vehicle, (c) resistivity of PI-A during the treatment at a condition of 130 °C, 85 RH%, and 3.3 V bias for 300 hours, (d) resistivity of PI-B during the treatment at a condition of 130 °C, 85 RH%, and 5 V bias for 100 hours.

IV. Conclusion

We have developed a polyimide capable of low-temperature curing for hybrid bonding. First, comparing several low-temperature curable polyimides on polishing rate by CMP, PI-A, and PI-B showed good polishing rates using alkaline slurry. By using these PIs, PI-PI bonding tests were carried out under low-temperature conditions and confirmed that they had sufficient bonding strength. Also, the mechanism of the PI-PI bonding process was examined through the surface free energy measurement and XPS analysis. Plasma treatment increased hydrophilic functional groups such as hydroxyl and carboxyl groups on the polyimide surface, which effected the polar component and hydrogen bonding component of the surface free energy increased. Based on these interactions of hydrophilic functional groups, strong joints of polyimides are formed by annealing after pre-bonding. Regarding physical factors, it is thought that sufficient PI-PI bonding can be achieved by meeting certain conditions of pressure and modulus of elasticity. The difference in the required bonding temperature between our developed two types of materials may be due to the difference in the modulus of elasticity at a certain temperature each other. Finally, the hybrid bonding of the PI/Cu chip and substrates using the developed polyimide material, PI-A, was demonstrated. All processes were proceeded and successfully completed at temperatures below 250°C without any void. Furthermore, PI-A and PI-B showed good reliabilities after B-HAST tests.

Acknowledgment

We would like to thank Advantec Co., Ltd. for R&D wafers provided and CMP for the polyimide substrates by AGC Inc. We also would like to thank the Institute of Microelectronics, Singapore's Agency for Science, Technology and Research, for providing Si substrates with copper pillars, conducting bonding tests, and observing cross-section views of hybrid bonding. Finally, we would also like to thank D-process Inc. for CMP on polyimide-copper substrates.

References

[1] Hong-Miao Ji, Lin Ji, Fa-Xing Che, Hong-Yu. Li, King-Jien Chui, M. Kawano, "Wafer Level High Density Hybrid Bonding for High Performance Computing," IEEE International Symposium on the Physical and Failure Analysis of Integrated Circuits (IPFA), 2020

[2] A. Jouve, V. Balan, N. Bresson, C. Euvrard-Colnat, F. Fournel, Y. Exbrayat, et al., "1µm pitch direct hybrid bonding with <300nm wafer-to-wafer overlay accuracy," IEEE SOI-3D-Subthreshold Microelectronics Technology Unified Conference (S3S), 2017

[3] A. Elsherbini, S. Liff, J. Swan, K. Jun, S. Tiagaraj, G. Pasdast, "Hybrid bonding interconnect for advanced heterogeneously integrated processors", IEEE 71st Electronic Components and Technology Conference (ECTC), 2021, pp.1014-1019.

[4] E. Bourjot, C. Castan, N. Nadi, A. Bond, N. Bresson, L. Sanchez, et al., "Towards 5µm interconnection pitch with Die-to-Wafer direct hybrid bonding," IEEE 71st Electronic Components and Technology Conference (ECTC), 2021, pp.470-475.

[5] F. Inoue, A. Phommahaxay, A. Podpod, S. Suhard, H. Hoshino, B. Moeller, et al., "Advanced dicing technologies for combination of wafer to wafer and collective die to wafer direct bonding," 69th Electronic Components and Technology Conference (ECTC), 2019, pp.438-445.

[6] S. P. S. Lim, S. C. Chong, V. Chidambaram, "Comprehensive study on Chip to wafer hybrid bonding process for fine pitch high density heterogeneous applications," IEEE 71st Electronic Components and Technology Conference (ECTC), 2021, pp.438-444.

[7] Jerome Panzer, "Components of solid surface free energy from wetting measurements," Journal of Colloid And Interface Science, vol. 44, 1973, pp. 142-161.